PAPER • OPEN ACCESS

The modeling of a tokamak plasma discharge, from first principles to a flight simulator

View the article online for updates and enhancements.

The modeling of a tokamak plasma discharge, from first principles to a flight simulator

E Fable[1,*] ⓘ**, F Janky**[1,4]**, W Treutterer**[1] ⓘ**, M Englberger**[1]**, R Schramm**[1] ⓘ**, M Muraca**[1]**, C Angioni**[1] ⓘ**, O Kudlacek**[1]**, E Poli**[1] ⓘ**, M Reich**[1] ⓘ**, M Siccinio**[1,2]**, G Tardini**[1]**, M Weiland**[1]**, C Wu**[3]**, H Zohm**[1] **and the ASDEX Upgrade Team**

[1] Max-Planck-Institut für Plasmaphysik, 85748 Garching, Germany
[2] EUROFusion, Garching bei Muenchen, Germany
[3] Karlsruher Institut für Technologie, Institute for Pulsed Power and Microwave Technology, Karlsruhe, Germany

E-mail: emiliano.fable@ipp.mpg.de

CrossMark

Abstract

A newly developed tool to simulate a tokamak full discharge is presented. The tokamak 'flight simulator' Fenix couples the tokamak control system with a fast and reduced plasma model, which is realistic enough to take into account several of the plasma non-linearities. A distinguishing feature of this modeling tool is that it only requires the pulse schedule (PS) as input to the simulator. The output is a virtual realization of the full discharge, whose time traces can then be used to judge if the PS satisfies control/physics goals or needs to be revised. This tool is envisioned for routine use in the control room before each pulse is performed, but can also be used off-line to correct PS in advance, or to develop and validate reduced models, control schemes for future machines like a commercial reactor, simulating realistic actuators and sensors behavior.

Keywords: tokamak, flight simulator, control, modeling, full discharge, theory

(Some figures may appear in colour only in the online journal)

1. Introduction

Magnetic confinement fusion is approaching the phase where electrical energy output will be obtained from a big-size burning plasma core. Thus, research in tokamak plasma modeling becomes increasingly important and is currently confronted with two major challenges. The first is provided by the preparation of the International Thermonuclear Experimental Reactor (ITER) operation [1], which will require the capability of simulating a complete plasma discharge directly from the pulse schedule (PS) before its actual execution, to test all possible aspects, particularly connected with control and safety. The second challenge is the design of a prototype tokamak fusion reactor (e.g. EU-DEMO, [2]), which requires the integration of technological and physical aspects with a high level of realism. Both major steps call for a solution in terms of integrated modeling allowing computationally fast but at the same time realistic and robust simulations of a complete plasma discharge.

The problem of the simulation of a complete plasma discharge is tackled by describing how the integrated numerical modeling of the tokamak system is constructed, moving from the external circuits and the machine vessel to the plasma core, highlighting both technological and physical aspects,
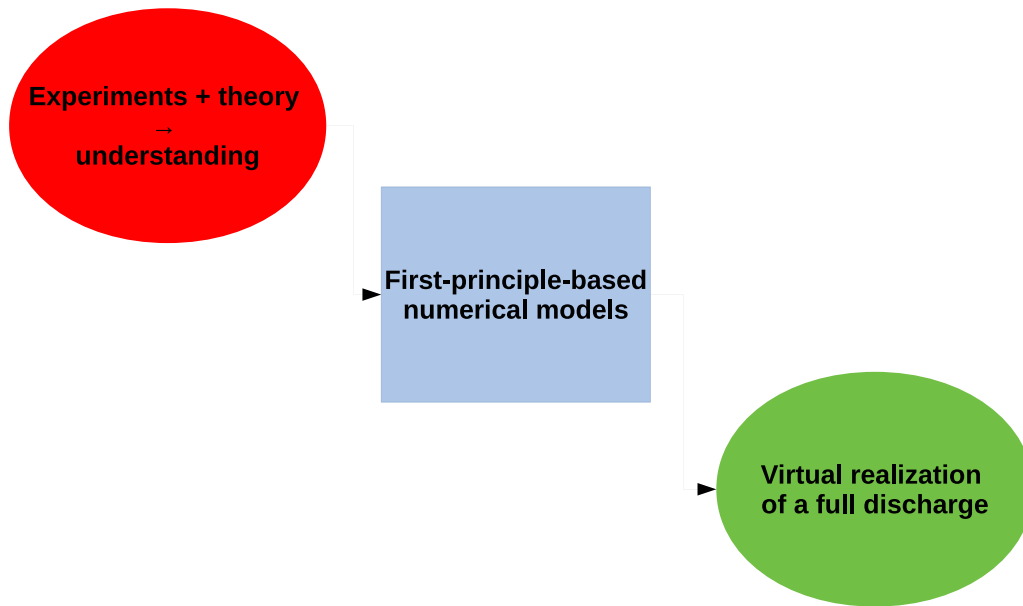
Figure 1. The 'trilogy' of fusion research.

as well as their interactions. The roles of these elements are also identified in the time evolution of the discharge, from the breakdown, to the plasma current ramp-up, the current flat top and the ramp down. The control requirements, which ensure operation inside prescribed limits, are strongly influenced by the interaction between the control system and the plasma response, the latter as an element of the complete tokamak electrical circuit, whose behavior cannot be simplified to a 0D entity due to profile effects and transport non-linearities. These need to be considered and integrated with a sufficient degree of realism in the description of the plasma response, including MHD limits, plasma transport, confinement transitions, interactions between plasma regions with closed and open field lines, as well as heating and fueling actuators physics. The path from present experimental and theory efforts to a full-discharge simulator is depicted in figure 1, which one could call a 'trilogy' which follows a logical order.

At this point the 'flight simulator' (FS) concept is introduced, with a distinguishing characteristic: its input is solely the machine description and the PS, i.e. the description of the trajectories, both feedforward or feedback, that the control system needs to ensure during the plasma discharge. It is the same document that the discharge control system (DCS) of the actual machine uses. The FS must simulate both the plasma and the control system. Moreover, it has to be fast enough to be run in-between discharge in the control room. This would allow a last check on programmed trajectories with respect to either the control requirements (limits) or the physics goals. A depiction of the basic blocks of the FS is given in figure 2.

The first-of-its-kind flight simulator Fenix [3–5], developed at ASDEX Upgrade, integrates all these elements. The core of this flight simulator is the ASTRA transport modeling environment [6, 7]. In this paper, the application of Fenix to actual ASDEX Upgrade discharges is demonstrated, highlighting the physics investigations that can be performed with this tool. With application to a future fusion reactor (EU–DEMO),

several aspects of reactor design that are impacted by plasma physics and by the plasma non-linearities [8, 9] are studied, e.g. profile stiffness, which transfers to the so-called power degradation of confinement, or the feedback loop between seeding divertor impurities and dilution of the core plasma, which can be severe for a reactor working in a state of divertor detachment [10–13]. Moreover, the application to EU–DEMO will help in designing appropriate sensors and actuators for the future machine.

2. Path from basic theory to the flight simulator

Focussing on the plasma model of the FS, it is now discussed how to build it up using the knowledge that has been gathered both from theory and from the experimental observations.

The plasma model, being the plasma embedded in a quasi-static magnetic field, requires primarily an MHD equilibrium model that solves the free-boundary Grad–Shafranov equation and the circuit equations for the active and passive conductor elements. MHD equilibrium solvers have been available for a long time and it is one of the most robustly well-known aspects of the plasma. One of the challenges in this context is to make them fast enough to be close to real-time. This can be achieved either via parallelization or using state-of-the art numerical schemes.

After the discharge is started, when the electric field in the plasma chamber reaches some critical threshold, the avalanche ionization process is initiated, and the plasma is formed. This phase, the 'breakdown' and the subsequent 'burn-through' phase, are extremely complex in terms of the elements that interact, and the feasibility of numerical description. As such, most models rely on simplified semi-empirical elements that need constant adjustment and offer little predictive power. The solution adopted in Fenix is to compute the chamber loop voltage as $V_{loop} = d\Psi_{coils}/dt$, where Ψ_{coils} is the
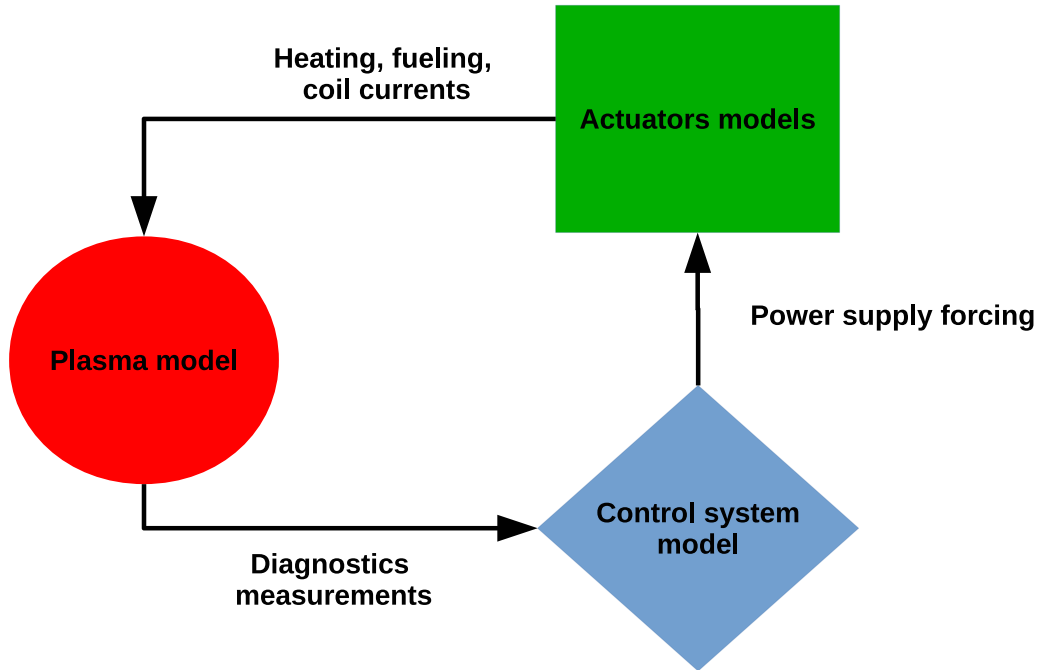
Figure 2. Simplified schematics of a flight simulator workflow.

poloidal flux produced by the active coils in the middle of the chamber. When $V_{loop} \approx 10$ V (based on a database of discharges), then a simple plasma current evolution equation is solved: $L_p dI_p/dt + R_p I_p = V_{loop}$, with L_p, R_p respectively plasma inductance and resistance fitted on a database of discharges on average. Initial condition for I_p is 1 A, and when it reaches 100 kA (arbitrarily defined), the full plasma–equilibrium solver are called. As such, this model does not predict breakdown success rate or burn-through physics. To add predictive capability to this simple model, much more has to be done, from describing the avalanche process to the burn-through phase and plasma motion in the early phase when quasi-static equilibrium is not stable.

For the core plasma different models are employed. Regarding temperature profiles (of electrons and ions), a simple gyro–Bohm scaling is used: $\chi_{gB} \sim \frac{T^{3/2}\sqrt{M}}{B^2 R}$. This forms the basis for assigning the heat diffusivities to electrons and ions, where the general form is $\chi_{e,i} = \chi_{gB} f_{e,i}(geom, T_e/T_i, q, s, \nu, \beta, \ldots) + \chi_{e,i}^{neo}$. The free coefficients are fitted such as to give observed core confinement on a selected database of discharges. For particle transport, a similar approach is used, but additionally convection terms are also defined such as to lead to peaked density profiles in realistic conditions. Reduced models for MHD activity like sawteeth or NTM are also included. Plasma radiation is computed using Bremsstrahlung formulas and analytical cooling factors [15]. Future development will add TGLF and QualiKiZ NN (Neural-Network) [14, 16, 17] to the choice of core transport models. Obviously the non-neural network version of the two codes can be used off-line when computational time is less of an issue.

The pedestal region, defined as a fixed radial interval, is modeled by assigning a fixed diffusivity in L-mode, while in H-mode, the diffusivity is scaled such as to maintain the pedestal top pressure at or below this critical value: $P_{ped,crit} = 0.33 R^{-0.38} e^{5\delta} I_p^{1.25} k^{0.62} \beta_N^{0.43}$ [18]. H-mode is achieved when the ion heat flux crossing the pedestal top equals this scaling: $Q_{i,ped} = 0.0011 n^{1.07} B_T^{0.76} S$ [19].

The SOL–divertor regions are modeled for exhaust, and particle balance (0D model for density evolution including gas puff source and pump sink). This particle balance model is new and has been coded specifically for Fenix. The exhaust model is built from a 1D heat dissipation equation, along a narrow flux tube running from an up-stream mid-plane location down to the divertor targets [13]. This model coincidentally reproduces a scaling proposed in [20], for the amount of impurities needed to reach detachment.

3. The flight simulator Fenix

Fenix has been obtained by embedding the ASTRA transport solver into Simulink-based PCSSP platform [21]. For now it has been developed to perform kinetic/magnetic control on ASDEX Upgrade (AUG) Tokamak, and kinetic control on DEMO tokamak. A core part of the flight simulator is the 'Plasma Model' (PM), which is the block that solves for the plasma dynamics and the plasma state, given the actuator commands (injected power, fueling, and coil currents). The PM in Fenix is the ASTRA code, coupled to the SPIDER equilibrium solver. The reduced models used have been described in the previous section. Both the plasma equilibrium (Grad–Shafranov equation) and the evolution of the coil currents are solved for in the SPIDER code [22], coupled to ASTRA. In figure 3 the workflow elements are shown. Notice that an 'ICRH' block, modeling heating from ion
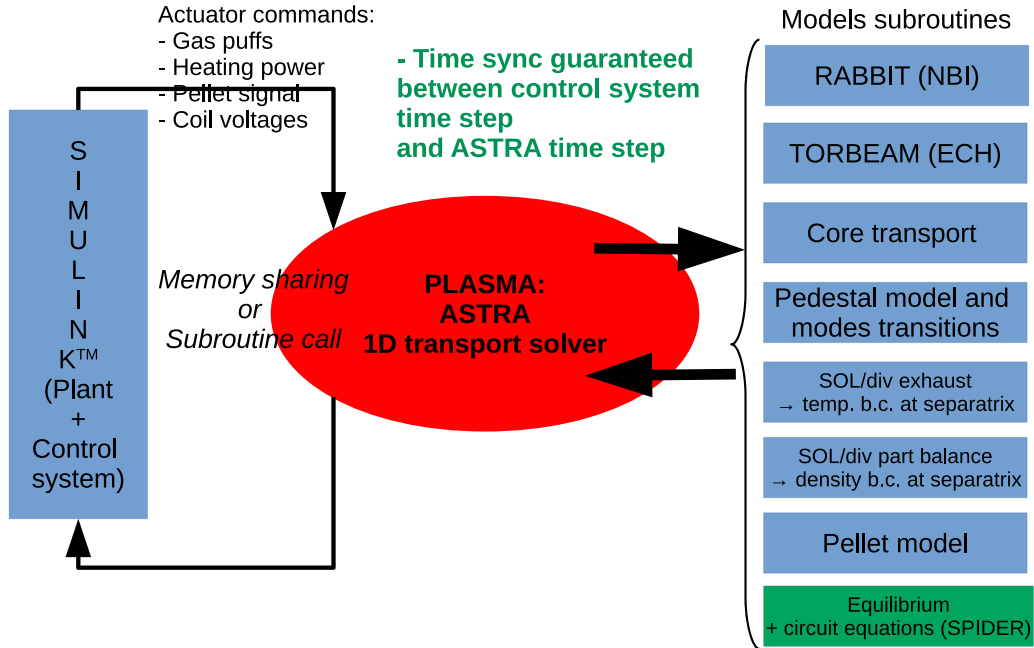
Figure 3. Detailed schematics on the Fenix workflow components. RABBIT [23] and TORBEAM [24] are coupled through external libraries.
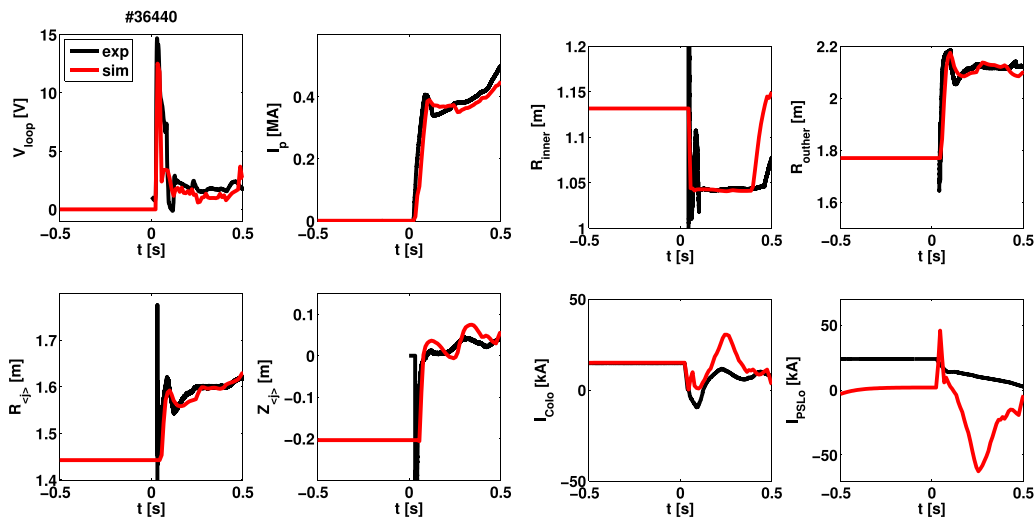
Figure 4. Time traces of several quantities, comparing experimentally measured (black, 'exp') and simulated (red, 'sim'). In order: separatrix loop voltage V_{loop}, plasma current I_{p}, inner major radius R_{inner}, outer major radius R_{outer}, current centroid major radius $R_{<j>}$, current centroid vertical position $Z_{<j>}$, current flowing in the CoIo active control coil I_{CoIo}, current flowing in the upper stabilizing coil I_{PSLo}.

cyclotrion resonance frequency waves, is absent, as reduced models for ICRF heating are not yet easily available.

4. Fenix for AUG

4.1. Sectioning a full-discharge simulation

In figure 4, the no-plasma to plasma transition (breakdown phase) is zoomed in, taken from a full-discharge simulation for discharge #36440. The breakdown is obtained at around $t \approx 25$ ms, while the first plasma equilibrium is computed at $t \approx 50$ ms when $I_{\text{p}} = 100$ kA. The limited $\rightarrow$ lower single

null (LSN) configuration transition is produced at $t \approx 0.35$ s, mainly driven by the coils that sit below the divertor targets. While the controlled traces and some of the derived ones are well matching the experimental measurements, one observes big deviations in the control currents 'IcoIo' and the passive stabilizing loop current 'Ipslo' in the time range $t < 0.45$ s. This discrepancy is supposed to be coming from missing stabilizing mechanisms arising from currents flowing on the open field lines, which are not modelled. Clarifying this will be the focus of a future work. In figures 5 and 6, two more sections of the ramp-up/flat-top phases are shown. At $t \approx 1.2$ s, the control system starts to control the strike-points position, which
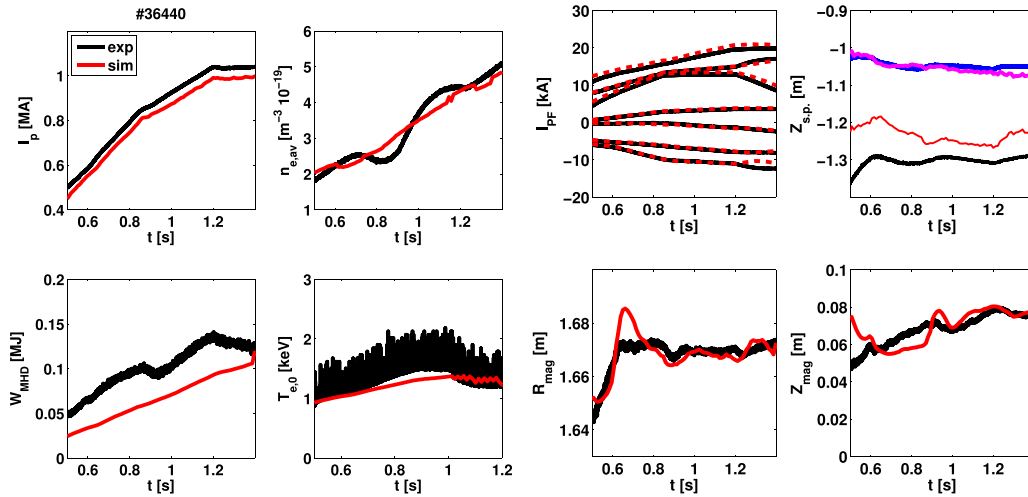
Figure 5. Analogous to figure 4 for the time interval $t = [0.5, 1.3]$ s. In the 4th panel, the black and blue colors are the experimental data for the two strike points locations (inner and outer target), while red and magenta are respectively from the simulation (inner and outer target). In order: plasma current I_p, average electron density $n_{e,avg}$, currents flowing in the poloidal field coils I_{PF}, strike points vertical positions $Z_{s.p.}$, plasma energy W_{MHD}, central electron temperature $T_{e,0}$, magnetic axis coordinates R_{mag}, Z_{mag}.
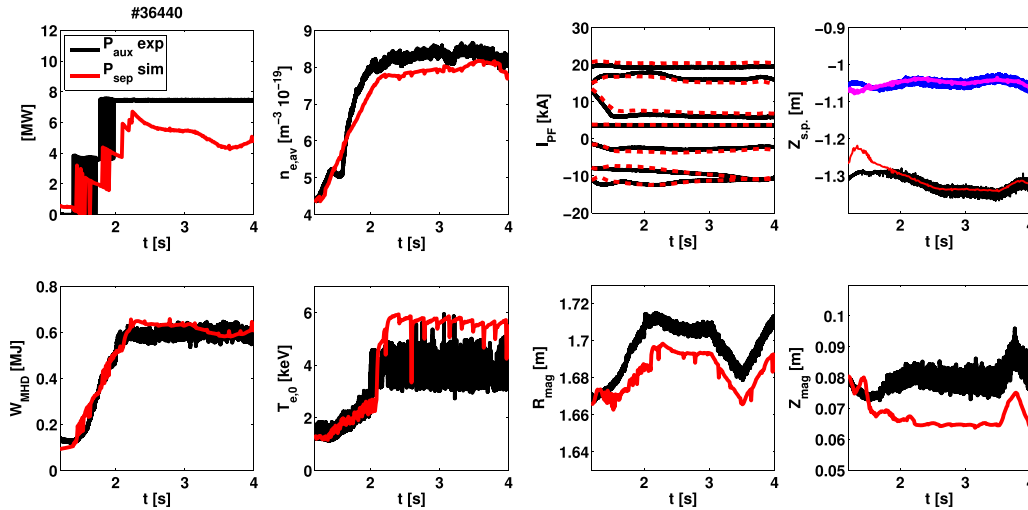
Figure 6. Same as figure 5, but for the time interval $t = [1.3, 4]$ s. In order: net power absorbed by the power (black injected, red absorbed), average electron density $n_{e,avg}$, currents flowing in the poloidal field coils I_{PF}, strike points vertical positions $Z_{s.p.}$, plasma energy W_{MHD}, central electron temperature $T_{e,0}$, magnetic axis coordinates R_{mag}, Z_{mag}.

appear then to be matching the experimental reconstruction. In turn, this means one has to check the quality of the simulated coil currents, which also match the experimental values rather well. Before the strike-point control is initiated, there is a discrepancy in the inner target (red vs black). Later this discrepancy disappears because the strike points are controlled actively (as such there could be a discrepancy on the coil currents that control them, but this discrepancy is small). The reason for the discrepancy in the early, non-controlled phase, maybe due to the edge current profile not being fully realistic (because the strike points depend strongly on the X-point structure which is mostly determined by the edge current density). The L–H transition happens at around $t \approx 1.5$ s, after which the plasma is in a stationary phase from the point of view of balance between sources and sinks. A test radial sweep is performed in the range

$3 < t < 4$ s, which shows that the simulations reproduces what is done in the real experiment.

4.2. Effect of edge plasma current on control coils currents

The prediction of the coil current evolution when the strike-points positions are controlled, relies on the shape of the X-point region, that is the shape of the current layer close to the separatrix. In turns, this means the physics of current evolution in the pedestal region during the H-mode operation. In figure 7, a case with full bootstrap current as obtained from formulas [25] is compared with a case where the bootstrap current is reduced, until the internal inductance l_{i3} is matched with the experimental reconstruction. When the internal inductance is matched, so are the coil currents. This shows that correct
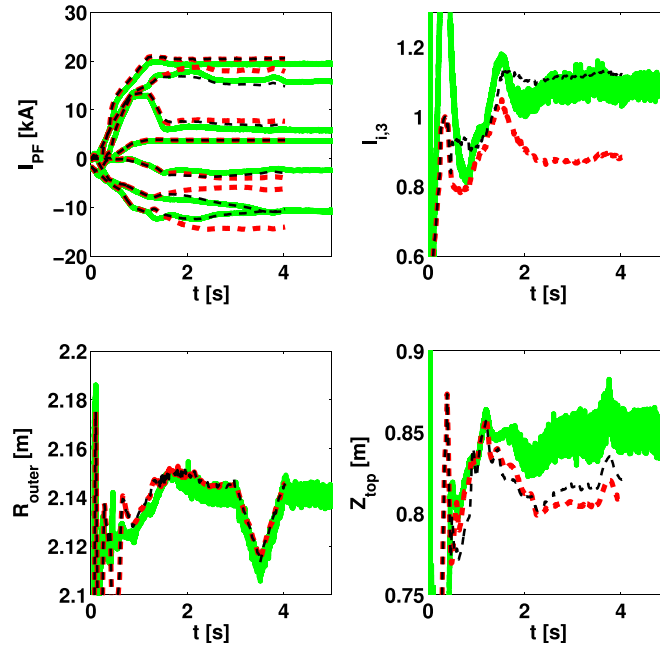
Figure 7. Time traces of PF coil currents (top–left), internal inductance (top–right), outer major radius (bottom–left), top vertical position (bottom–right). In solid green: experimental estimates. In dashed red: case with full edge bootstrap current. In dashed black: case with reduced edge bootstrap current.

prediction of the physics of the edge current layer is fundamental to predict the coil currents evolution. The fact that the bootstrap current has to be reduced, is consistent with the presence of strong ELMy activity. In future work, a more predictive model for this effect should be produced.

4.3. Modeling fueling and density evolution

In figure 8, the focus is on the evolution of the plasma density, both in the core and in the SOL/divertor regions. Since the core plasma density is a control quantity, the control system will deliver as output command for the gas puff (divertor valve for D). The results show that the predicted gas puff in p/s is matching the experimental value in trend and in magnitude (with discrepancy arising from not-yet-fully calibrated model constants). The trend, which shows that separatrix density scales roughly as gas puff to power 1/3, is consistent with results from [26]. The simulation also predicts neutral density at plasma separatrix, which is in the order of 2–$3 \cdot 10^{15}$ m^{-3}, and ratio of divertor to SOL density, simulated in the order of ~ 30, again consistent with estimates presented in [26].

4.4. Modeling a discharge with complex shape evolution

Finally, the simulation of a discharge where several shape/mode transitions occurred, is presented in this sub-section. Discharge #36026 has been the first trial in AUG to push the plasma shape towards negative triangularity, particularly by playing with the upper triangularity. The results of the Fenix simulation for this discharge are shown in figure 9, where several time traces are shown, comparing model and experiment. It can be seen that Fenix reproduces with good
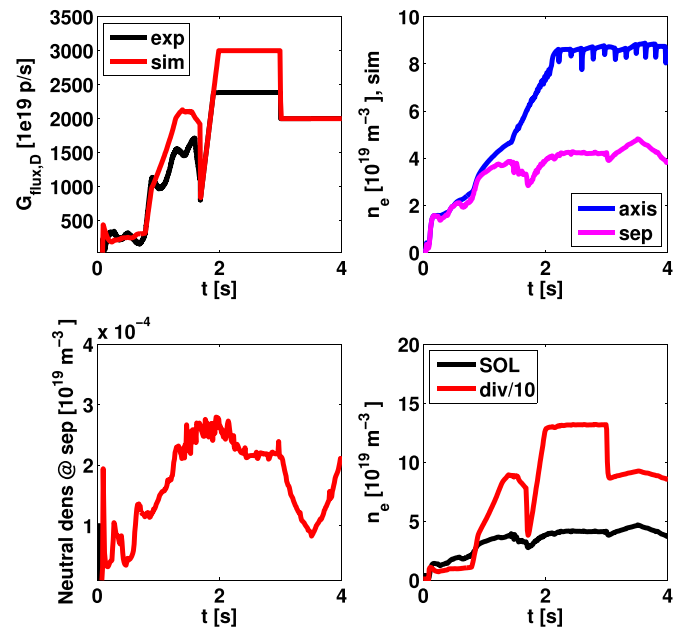
Figure 8. Time traces of gas puff (top–left), simulated density (top–right), simulated neutral density (bottom–left), and simulated density outside of the plasma (bottom–right).

accuracy many features of the experiment, except for the late surge in plasma density (at around $t \approx 5.5$ s, where the simulation instead predicts a drop in density. On the other hand, the plasma energy evolution is well captured. The sequence of equilibria observed during the discharge evolution are pictured in figure 10, plotting several time slices. While the agreement between simulated and reconstructed equilibria is very
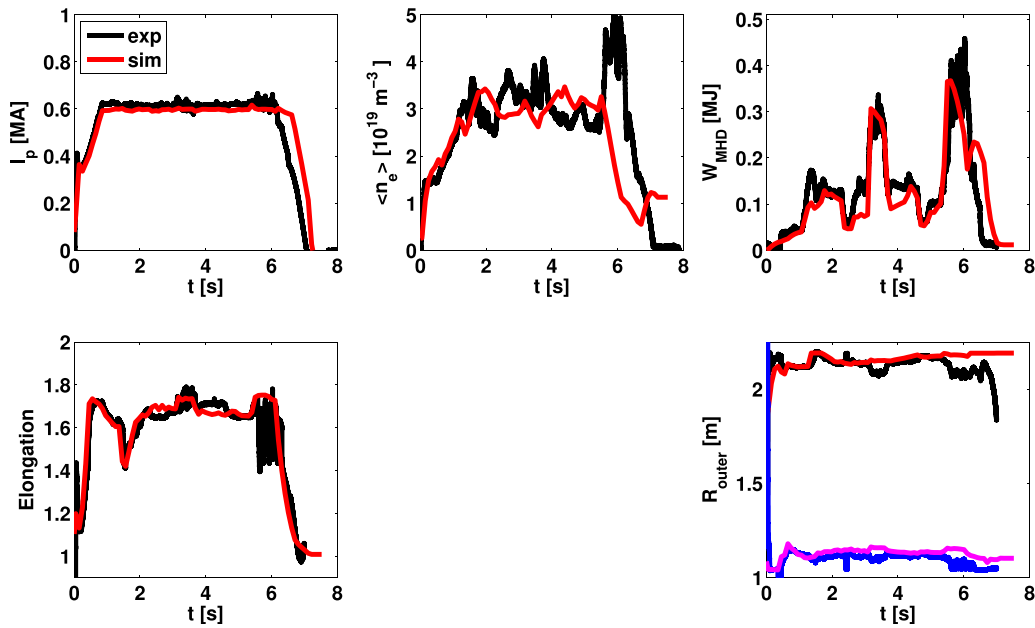
Figure 9. Time traces of a simulated negative triangularity discharge (#36026). In the 5th panel, the blue and magenta lines are respectively experimental and simulated data for the innermost major radius point of the plasma.

good up to 3 s, it is observed that the simulation predicts an outer limited plasma, while the experimental reconstruction displays an inner limited plasma. The origin of this discrepancy is not known yet. Both phases where the discrepancy is observed are in H-mode (in the simulation as in the experiment). So, despite having similar energy, the simulation and the experiment show completely different behavior. One possibility could be the shape of the profiles, which have a great influence on the equilibrium especially in H-mode (at higher–beta, profiles influence equilibrium more than at low–beta).

5. Fenix for EU–DEMO

In this section, one example of modeling using the Fenix flight simulator for EU–DEMO is presented.

5.1. Effect of pellet fueling on EU–DEMO plasma stability

One of the key results obtained using Fenix for EU–DEMO has been to show the sensitivity of the scenario to a whole zoology of perturbations, either intrinsic to the plasma (transport, MHD, mode transitions), or coming from the outside (e.g. loss of auxiliary heating, failure of the pellet system). One such case is displayed in figure 11, where the focus is on the realism of the pellet injector system. As it is known, every now and then a pellet is missed from delivery due to various technical and physical causes. As such, pellet success rate of injection cannot be 100%. In the simulation presented, success rate is assumed to be 90%, which is in line with present technological capabilities. The simulation shows that the plasma undergoes long-time scale fusion power oscillations, which are precisely induced by a pellet missed.

It is also found that missing a pellet will have an effect on the SOL/divertor region, because of the variation in density, and the outgoing particle/heat wave from the plasma into the SOL region. This in turn will force the control system to react with a sudden puff of Ar to maintain detachment and divertor protection at all times. Doing this work, it is found that a feedforward (FF) Ar injection strategy (e.g. injecting constant Ar puff such as to cushion out all perturbations) is better than relying on a feedback (FB) strategy (Ar puffed correlating with some control parameters). This is shown in figure 12, where a comparison is made between FF and FB strategies.

The reason why the FF strategy is better is due to the control parameter itself. For detachment, several candidates could be considered. However, none of them is sufficiently reliable. For example: electron temperature in front of the divertor, which is extremely non-linearly dependent on the local impurity content, radiation characteristics, and fueling. Specifically, as observed in present experiments, it is not yet clear how to identify detachment or attachment based on some continous change in a parameter, which is smooth enough to be able to control it. Although recently focus has been put on the X-point radiator being a good proxy for SOL/divertor cooling, development is still needed before a robust control scheme for detachment can be developed and ported to DEMO. That is why we now prefer to stick to a FF strategy, which has the advantage of being less reliant on the actual physics mechanisms and their non-linearities.

In the framework of the EU–DEMO development at EUROFusion, this tool is going to be used more systematically to design actuators and sensors including the most realistic behavior possible.

It is also worth noting that a similar work was conducted for ITER in [27], where it was found that pellet injection has a direct impact on the SOL/divertor attached/detached state
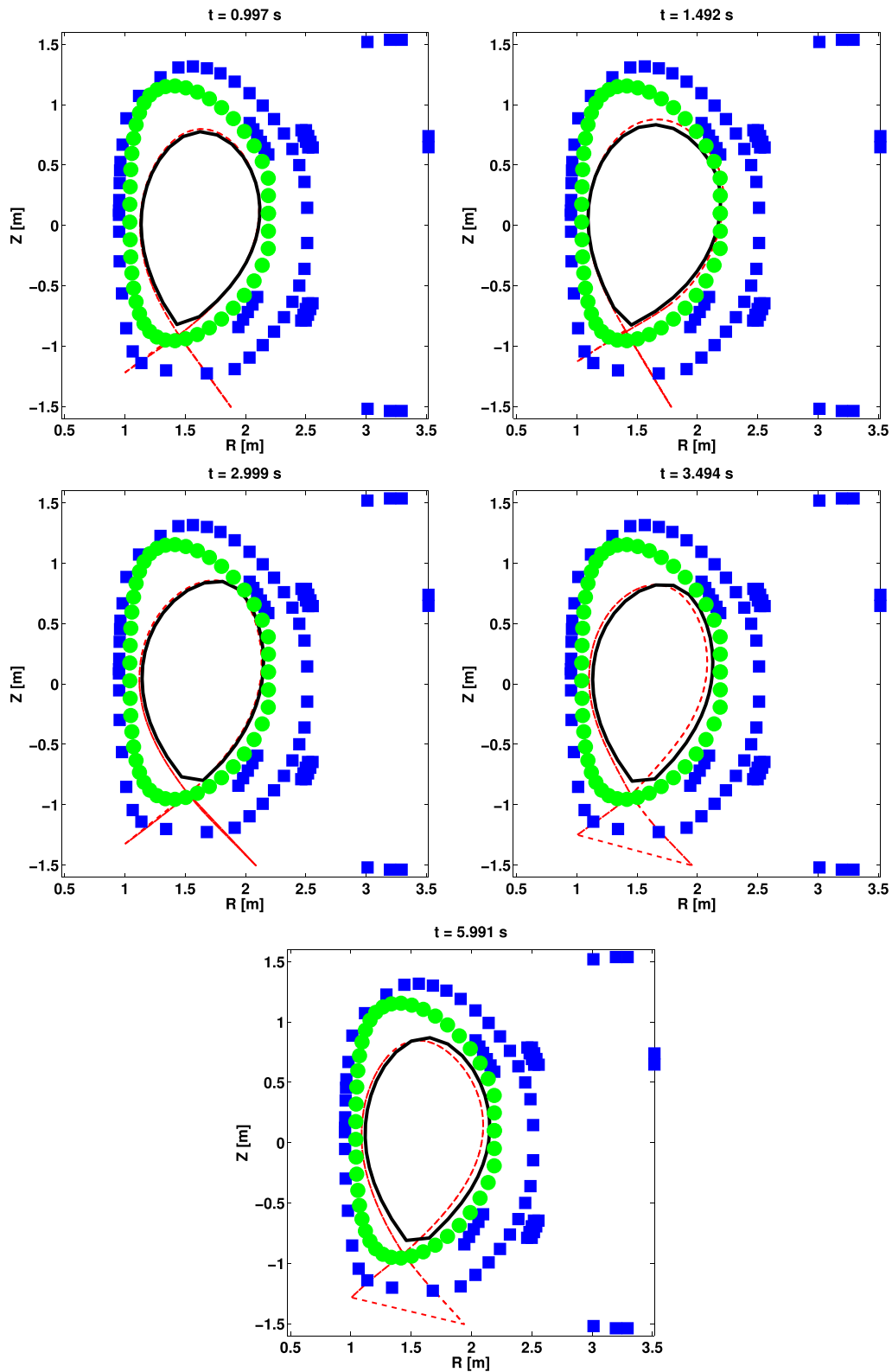
Figure 10. Evolution of the boundary shape (black—simulated, red—reconstructed) for the negative triangularity discharge. In green dots: the limiter contour. In blue squares: passive conducting elements.
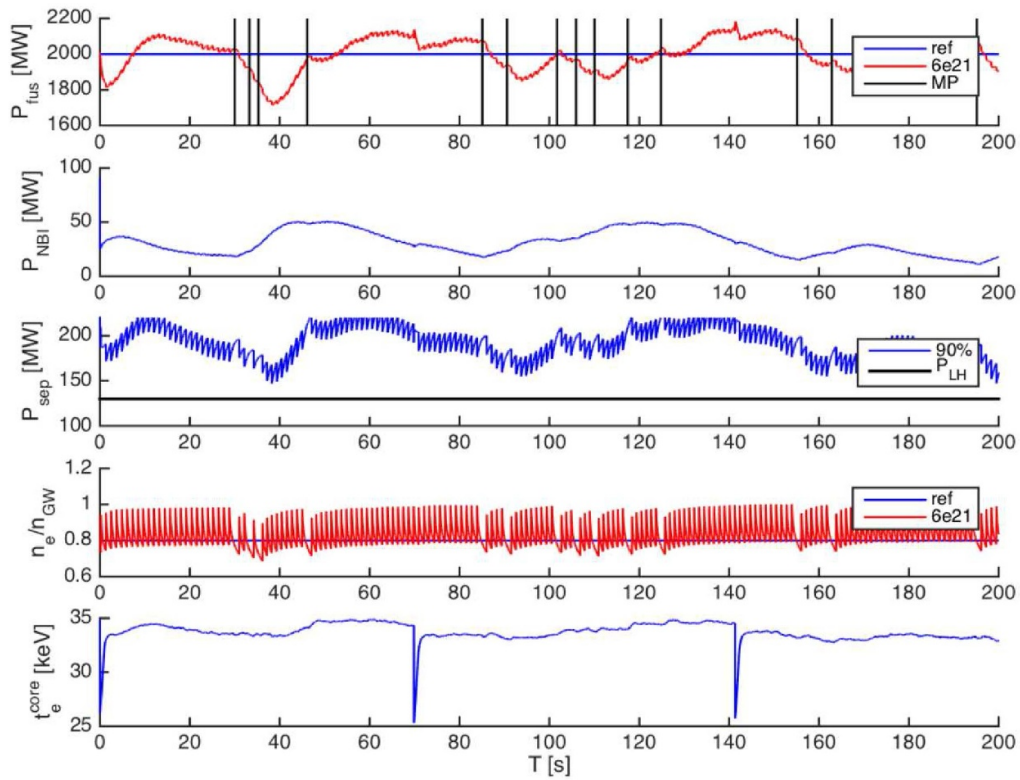
Figure 11. Time traces of fusion power (panel 1), NBI power (panel 2), separatrix power (panel 3), pedestal top Greenwald fraction (panel 4) and central temperature (panel 5) for the baseline EU–DEMO run. Vertical lines in panel 1 indicate the time in which a pellet is missed (i.e. is lost in the delivering tube). The events in central electron temperature (bottom panel) at $t \approx 70s$ and $t \approx 140$ s are sawtooth crashes.
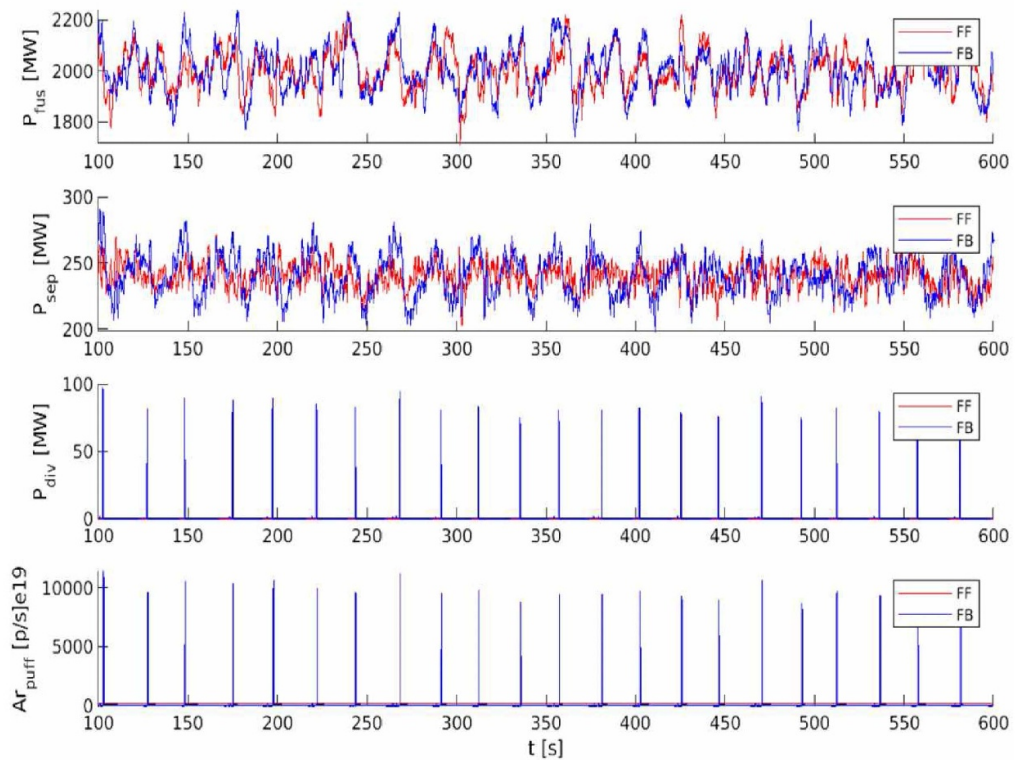
Figure 12. Time traces of fusion power (panel 1), separatrix power (panel 2), divertor power (panel 3) and Ar puff (panel 4) for both feedforward (red) and feedback (blue) Ar delivery strategy.

dynamics, due to the intermittent heat waves caused by each pellet via the convective flux term in the energy continuity equation. This could be another motivating factor in establishing a more robust detachment control scheme which can cushion out all these intermittent perturbations.

6. Conclusions

In this work, the flight simulator Fenix is presented, focusing on the physics models and results that display some of the possible physics applications on ASDEX Upgrade and EU–DEMO.

For AUG: Fenix has so far been used to test some of the physics models, the interaction of the control system with the plasma, and the behavior of the full system. It is planned in the near future to start to use it routinely in the control room and for full-discharge prediction, validation of reduced physics models, and development of better physics and control models (actuators and synthetic diagnostics).

For EU–DEMO: it is shown that kinetic control using realistic actuator behavior (e.g. the pellet injector) can be optimized to avoid unwanted oscillations in the fusion power or loss of detachment due to density perturbations.

These are just a few examples of the many applications of the Fenix flight simulator.

Data availability statement

The data that support the findings of this study are available upon reasonable request from the authors.

Acknowledgments

ORCID iDs

E Fable ● https://orcid.org/0000-0001-5019-9685
W Treutterer ● https://orcid.org/0000-0003-0268-1578
R Schramm ● https://orcid.org/0000-0002-9118-4575
C Angioni ● https://orcid.org/0000-0003-0270-9630
E Poli ● https://orcid.org/0000-0001-7552-4800
M Reich ● https://orcid.org/0000-0001-9029-5647

References

[1] (Available at: www.iter.org)
[2] Federici G *et al* 2017 *Nucl. Fusion* **57** 092002
[3] Janky F *et al* 2017 *Fusion Eng. Des.* **123** 555
[4] Janky F *et al* 2019 *Fusion Eng. Des.* **146** 1926–9
[5] Janky F *et al* 2021 *Fusion Eng. Des.* **163** 112126
[6] Pereverzev G V and Yushmanov Y P 1991 *IPP Report 5/42*
[7] Fable E *et al* 2013 *Plasma Phys. Control. Fusion* **55** 124028
[8] Fable E *et al* 2018 *Fusion Eng. Des.* **123** 555
[9] Fable E *et al* 2019 *Nucl. Fusion* **57** 066046
[10] Pütterich T *et al* 2019 *Nucl. Fusion* **59** 056013
[11] Siccinio M *et al* 2018 *Nucl. Fusion* **58** 016032
[12] Wenninger R *et al* 2017 *Nucl. Fusion* **57** 016011
[13] Siccinio M *et al* 2016 *Plasma Phys. Control. Fusion* **58** 125011
[14] Staebler G M *et al* 2017 *Nucl. Fusion* **57** 066046
[15] Post D E *et al* 1977 *At. Data Nucl. Data Tables* **20** 397–439
[16] Meneghini O *et al* 2017 *Nucl. Fusion* **57** 086034
[17] van de Plassche K L *et al* 2020 *Phys. Plasmas* **27** 022310
    Ho A *et al* 2021 *Phys. Plasmas* **28** 032305
[18] Kim S K *et al* 2018 *Nucl. Fusion* **58** 016036
[19] Schmidtmayr M *et al* 2018 *Nucl. Fusion* **58** 056003
[20] Reinke M L 2017 *Nucl. Fusion* **57** 034004
[21] Walker M L *et al* 2015 *Fusion Eng. Des.* **96–97** 716–19
[22] Ivanov A A *et al* 2005 *32nd Conf. on Plasma Physics* vol 29C (ECA) p -5.063
[23] Weiland M *et al* 2018 *Nucl. Fusion* **58** 082032
[24] Poli E *et al* 2018 *Comput. Phys. Commun.* **225** 36–46
[25] Sauter O and Angioni C 1999 *Phys. Plasmas* **6** 2834
[26] Kallenbach A *et al* 2018 *Plasma Phys. Control. Fusion* **60** 045006
[27] Wiesen S *et al* 2017 *Nucl. Fusion* **57** 076020